Korean J. Chem. Eng., 33(2), 507-513 (2016)
DOI: 10.1007/s11814-015-0164-1

pISSN: 0256-1115
eISSN: 1975-7220

Oxidation of ash-free coal from sub-bituminous and bituminous coals in a direct carbon fuel cell

Duc-Luong Vu and Choong-Gon Lee†

Department of Chemical and Biological Engineering, Hanbat National University,
125, Dongseodae-ro, Yuseong-gu, Daejeon 305-719, Korea
(*Received 23 January 2015 • accepted 30 July 2015*)

Abstract−The present study proposes the production of ash-free coal (AFC) and its oxidation as a primary fuel in direct carbon fuel cells (DCFCs). The AFC was produced by the extraction of Arutmin sub-bituminous coal (AFC1) and Berau bituminous coal (AFC2) using polar solvents such as *N*-methyl-2-pyrrolidone (NMP), *N*,*N*-dimethylacetamide (DMA), *N*,*N*-dimethylformamide (DMF) and dimethyl sulfoxide (DMSO). It was carried out at a temperature of around 202 °C under atmospheric conditions and using a microwave irradiation method. Using NMP as the solvent showed the highest extraction yield, and the values of 23.53% for Arutmin coal and 33.80% for Berau coal were obtained. When NMP was added to DMSO, DMA and DMF, the extraction yield in the solvents was greatly increased. The yield of AFC from a sub-bituminous coal was slightly lower than that from a bituminous coal. The AFC was evaluated in a coin-type DCFC with a mixture of AFC and carbonate electrolyte (3 g/3 g) at 850 °C. The AFC and gaseous H_2 fuels were compared using the electrochemical methods of steady-state polarisation and step chronopotentiometry. The DCFC ran successfully with the AFCs at 850 °C. The open-circuit voltages were about 1.35 V (AFC1) and 1.27 V (AFC2), and the voltages at 150 mA cm^{-2} were 0.61 V (AFC1) and 0.74 V (AFC2).

Keywords: Ash-free Coal, Solvent Extraction, Sub-bituminous Coal, Bituminous Coal, Molten Carbonate, Direct Carbon Fuel Cell

INTRODUCTION

Coal is an important energy resource in the world and is the most abundant fossil fuel. However, raw coal has a high ash content that limits its utilization. Therefore, the development of an ash-free coal (AFC) has been attempted and developed to extend its application [1-3]. One of the promising uses of AFC will be as a fuel for direct carbon fuel cells, and AFC must have a high surface area, large numbers of surface oxygen functional groups, and low ash content to meet the needs of DCFC [4-6].

AFC is generally produced by the solvent extraction method. During the extraction process, the organic material in coal is extracted into the solvent. The extraction is generally carried out with organic solvents such as *N*-methyl-2-pyrrolidone (NMP), 1-methyl naphthalene, quinolone and tetralin to produce AFC. Takanohashi et al. [7] reported that extraction yields higher than 73% were obtained for sub-bituminous coal at 360 °C with the polar industrial solvent crude methylnaphthalene oil (CMNO). Giray et al. [8] reported that extraction with NMP, NMP/ethylenediamine (EDA) (17 : 1 vol/vol) mixture and NMP/tetralin (9 : 1 vol/vol) mixture yielded ash content ranging from 0.11 to 1.10%. Moreover, they suggested that the ash content of the solid extract obtained through microwave extraction was less than that from thermal extraction. Shui et al. [9] showed the thermal dissolution (TD) behavior of Shenfu coal, which is a kind of Chinese sub-bituminous coal. They reported that almost all of the ash in the raw coal was transferred into the TD residue and that the TD soluble yield was increased by increasing the TD temperature from 300 to 360 °C, with 1-methylnaphthalene as solvent.

Direct carbon fuel cells (DCFCs) directly convert the chemical energy of solid carbon fuel into electricity with high efficiency [10, 11]. Various types of DCFCs have recently been investigated. They are categorized by the electrolyte used in the cell: alkaline, molten carbonate or solid oxide [12-14]. Among them, molten carbonates have received attention for practical use because of their high conductivity, good stability in the presence of CO_2 produced from the carbon electro-oxidation reaction and suitable melting temperature [15,16]. The molten carbonate electrolytes are a combination of K_2CO_3, Na_2CO_3 and Li_2CO_3. DCFCs based on molten carbonate electrolytes operate at high temperatures between 600 and 900 °C to achieve a high conductivity of the molten salt [17]. The carbonate ion, CO_3^{2-}, is considered to be the charge carrier.

The two reactions occurring within a DCFC with a molten carbonate electrolyte are given by Eqs. (1)-(4) [13,17]:

Anode reaction

$$C+CO_3^{2-} \rightarrow 2CO+O^{2-} \quad (1)$$

$$2CO+2CO_3^{2-} \rightarrow 4CO_2+4e^- \quad (2)$$

Cathode reaction

$$O_2+2CO_2+4e^- \rightarrow 2CO_3^{2-} \quad (3)$$

The total reaction

$$C+O_2 \rightarrow CO_2 \qquad E^o=1.026\ V\ (at\ 850\ ^oC) \quad (4)$$

†To whom correspondence should be addressed.
E-mail: leecg@hanbat.ac.kr

Table 1. Proximate and ultimate analyses of raw coal and ash-free coal

Sample	Proximate analysis (wt%, db)				Ultimate analysis (wt%, db)			
	Moisture	Ash	VM	FC	C	H	N	O
Raw - Sub bituminous coal	6.96	13.32	40.04	39.68	69.12	5.12	4.71	20.81
Raw - Bituminous coal	15.74	7.78	35.42	41.06	72.46	4.08	1.32	14.16
AFC - Sub bituminous coal	0.42	0.78	50.40	47.91	76.06	5.65	2.92	15.30
AFC - Bituminous coal	2.14	1.37	51.34	45.15	72.23	5.24	2.90	18.26

The reactant carbon and the product carbon dioxide exist as pure substances; therefore, their chemical potentials (activities) are fixed and independent of the extent of conversion of the fuel. This may allow a full conversion of the carbon fuel in a single pass with the theoretical voltage of the DCFC remaining nearly constant at around 1.02 V (from room temp. to 1,200 °C). However, experimental OCVs can be higher due to the properties of the carbons and gas concentrations. In particular, low CO_2 concentrations in the anode compartment under inert gas purge can result in an increased OCV, as discussed previously [16].

Recently, DCFCs based on AFC fuel have been reported by many researchers. Jeon et al. [6] reported the feasibility of using AFCs in solid-oxide-electrolyte DCFCs. The cell voltage was about 1.1 V in the temperature range 600-900 °C.

In the present work, the production of AFCs from Arutmin sub-bituminous and Berau bituminous coal is investigated by using microwave irradiation (MI) at 202 °C under atmospheric pressure conditions. In addition, the oxidation behavior of AFC was investigated by the electrochemical methods of steady-state polarization, step chronopotentiometry (SC) and open-circuit voltage (E_{OCV}) measurement at 850 °C.

EXPERIMENTAL

1. Coal Samples

Indonesian sub-bituminous coal, Arutmin coal and Berau bituminous coal were used in this study. The coal samples were ground and sieved to give a particle size of less than 200 μm. They were stored under a nitrogen atmosphere and dried for 12 h under vacuum at 80 °C before use. The ultimate and proximate analyses of the Arutmin coal and Berau coal are shown in Table 1. The solvents used in this study were NMP, *N,N*-dimethylacetamide (DMA), *N,N*-dimethylformamide (DMF) and dimethyl sulfoxide (DMSO), all of which were purchased from Sigma Aldrich Co.

2. Microwave Extraction of Coal

The coal was extracted at atmospheric pressure in a round-bottomed glass flask fitted with a reflux condenser. A microwave oven with a variable power supply of 800 W (maximum) was employed. A schematic diagram of the microwave oven used for the coal extraction is shown in Fig. 1. The flask was charged with the coal and a polar solvent at different solvent-to-coal (S/C) ratios and then heated. The temperature inside the flask was kept at approximately 202 °C, which is the boiling point of NMP. To determine the effect

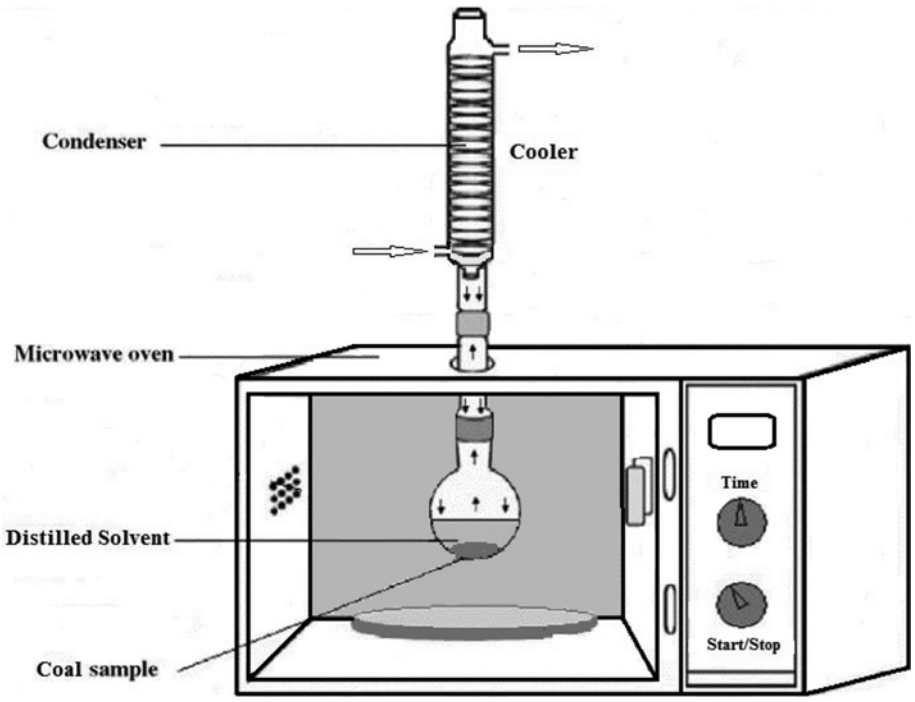

Fig. 1. Representation of the modified microwave oven for the AFCs.

of the ratio of the volume of solvent (mL) to the mass of coal (g), 140 ml of solvent was used and the S/C ratios were varied between 7 : 1, 14 : 1 and 28 : 1. After extraction, the flask was cooled to room temperature, at which point the solid residue and liquid phases were separated by filtration after centrifugation for 30 min at 10,000 rpm. The residue was washed with deionized water until the filtrate became almost colorless, and then it was dried under vacuum at 80 °C for 12 h. The extraction yield is defined as follows:

$$\text{Extraction yield [wt\%, daf]} = \frac{1-\frac{\text{Residue [g]}}{\text{Feed coal [g]}}}{1-\frac{\text{ash [wt\%]}}{100}} \times 100 \quad (5)$$

After the liquid phase was dried under vacuum at 170 °C for 40 h, the AFCs were obtained. AFC1 was made from a sub-bituminous Arutmin coal and AFC2 from a bituminous Berau coal.

3. Analyses of Products

The characterization of the AFCs and coal samples was carried out using the ASTM method. The functional groups were detected by Fourier-transform infrared spectroscopy (FT-IR; Nicolet 6700, Thermo Electron). X-ray diffraction (XRD) patterns were also obtained (DMAX-2500, Rigaku). The proximate analysis (ASTM D 5142-02a) was performed by using a thermo-balance (TGA/SDRA51e, Mettler Toledo) instrument. Ultimate analysis was performed according to ASTM D 5373-02 (EA1108, Thermo Scientific).

4. DCFCs

A schematic drawing of a coin-type DCFC system is illustrated in Fig. 2. The anode was a porous Ni-Al metal sheet and the cathode was a porous Ni sheet. The matrix was made of $LiAlO_2$ and the electrolyte contained 62 mol% Li_2CO_3+38 mol% K_2CO_3. The electrodes and matrices were supplied by the Korean Electric Power Research Institute, which developed the molten carbonate fuel-cell system. The carbonates were of reagent grade. Silver wire was used for the cathode leads, whereas Ni wire was used for the anode leads.

The cell was installed without carbon fuel in a box furnace that had a hole to penetrate the upper side of the alumina tube at the anode. The temperature of the cell in the furnace was initially raised by 2 °C min^{-1} from room temperature to 350 °C in air. Subsequently, the temperature was increased to 850 °C. During the temperature ramp, a mixture of 70 mol% air and 30 mol% CO_2 was supplied to the center of the cathode at a rate of 0.200 L min^{-1}, and a mixture of CO_2 (0.100 L min^{-1}) and H_2 gas (0.015 L min^{-1}) was introduced to the anode. When the cell temperature reached 850 °C, a mixture of H_2 (0.125 L min^{-1}) and CO_2 (0.025 L min^{-1}) was supplied through the deionized water bubbler to the anode to ensure cell performance. Then, the hydrogen fuel was interrupted and AFC fuel was introduced into the anode with nitrogen gas purging.

A mixture of 3 g of AFC and 3 g of molten carbonates (62 mol% Li_2CO_3+38 mol% K_2CO_3) was placed in an alumina tube of 1.5 cm in diameter and 10 cm in length. Both ends of the alumina tube were plugged with Ni foam. This alumina tube was placed in a larger alumina tube. Both of the alumina tubes were put into the furnace, one end of the larger alumina tube being plugged with glass wool. More details of the cell preparation and operation have been described in previous works [13,17].

The performance of the cell was measured with a potentiostat (PARSTAT 2273, Princeton Applied Research), which was operated with Power Suite software. The electrochemical methods employed in this work were E_{OCV} measurements, steady-state polarisation and SC. In the SC measurement, the current was raised from 0 to 150 mA cm^{-2} in 50 mA cm^{-2} steps for 60 s, and the subsequent potential relaxations were recorded.

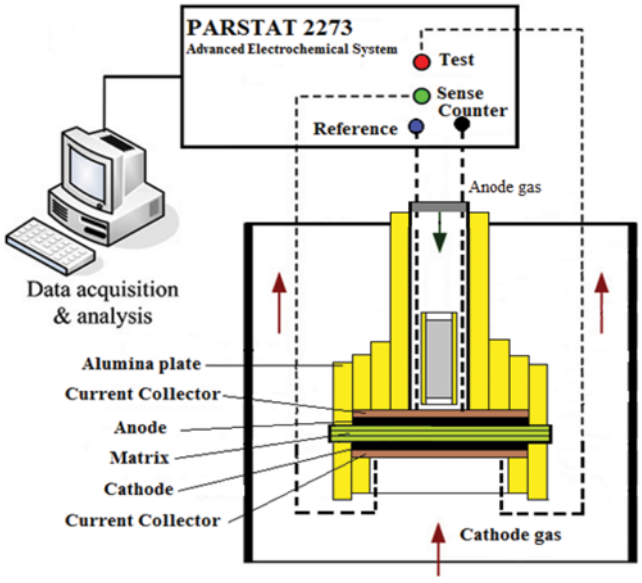

Fig. 2. Schematic drawing of a coin-type DCFC system.

RESULTS AND DISCUSSION

1. Extraction of AFCs

The effects of various polar solvents on the extraction yield at 202 °C are shown in Fig. 3. In this experiment, mixtures with NMP, such as DMF+NMP, DMSO+NMP and DMA+NMP, were prepared by the addition of 20 vol% NMP into various polar solvents. The extraction yield of 23.53 wt% with NMP is the highest among the solvents employed here, which is higher by 5.31, 10.84 and 9.92 wt% than that with DMF, DMSO and DMA, respectively. During the extraction of the coals with an organic solvent, the solvent pene-

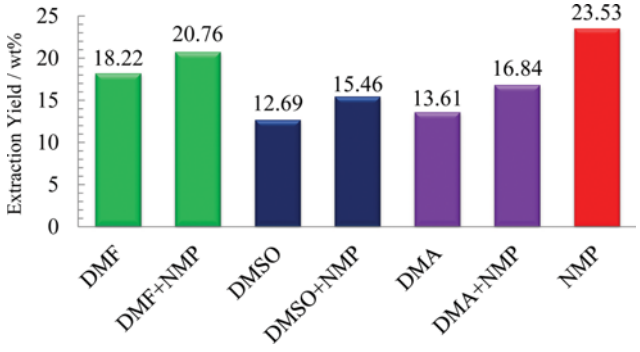

Fig. 3. The extraction yields of Arutmin sub-bituminous coal after 10 min MI in various solvents at 202 °C. The numbers above the bar are the extraction yields of the solvents. The mixtures were prepared by adding 20 vol% of NMP into each solvent.

Table 2. Extraction yields of sub-bituminous and bituminous coals with various solvent-to-coal (S/C) ratios and microwave irradiation times using 140 ml of NMP

	Extraction yield/ wt%					
	5 min		10 min		20 min	
S/C ratio	Bituminous	Sub-bituminous	Bituminous	Sub-bituminous	Bituminous	Sub-bituminous
28/1	33.80	19.15	25.90	22.63	32.30	23.77
14/1	20.82	18.12	18.42	21.32	21.57	22.25
7/1	14.70	10.44	14.70	12.28	18.67	13.44

trates the coal matrix and breaks the various non-covalent interactions such as van der Waals forces, hydrogen bonds, charge-transfer complexes, π-π interactions and ionic forces [1,7]. NMP is a strong polar solvent that acts as a good hydrogen bond acceptor when it is used as an extraction solvent. It has been suggested that NMP cleaves ionic forces and hydrogen bonds between the coal matrices, thus increasing the extraction yield [8]. NMP can swell the macromolecular structural network of coal through π-π interactions, owing to its naphthalene ring, which promotes the diffusion of the soluble fractions inside the network structure into the solvent [1,2]. Therefore, hydrogen bonds can be released between OH groups. This will result in the extraction yield being slightly higher when 20 vol% NMP is added to three of the solvents (DMF, DMSO, DMA). The extraction yields of DMF+NMP, DMSO+NMP and DMA+NMP were 20.76, 15.46 and 16.84%, respectively. The increased solubility of the mixed solvent systems may be attributed to synergistic effects, which render more of the extractable sites accessible to NMP and increase its ability to disrupt specific hydrogen bonds and ionic interactions in coal, thereby resulting in greater solubilization.

Samples of bituminous and sub-bituminous coals were exhaustively extracted with different S/C ratios and different extraction times. The results are presented in Table 2, which shows that for all of the coals, the extraction yield of NMP under microwave irradiation (MI) increases with an increase in S/C ratios. In addition, the bituminous coal was found to have a relatively higher extraction yield than that of sub-bituminous coal. The bituminous coal with an S/C ratio of 28 : 1 and with an extraction time of 5 min exhibited a maximum extraction yield of 38% [18]. The extraction yields of sub-bituminous coal with NMP increased with increasing extraction time, and the highest extraction yield was 23.77% when the S/C ratio was 28 : 1 with an extraction time of 20 min. The difference in the extraction yields between bituminous and sub-bituminous coal was attributed to the carbon content of the coals. The extraction yield rises with increasing carbon content. The carbon content is about 72.46% in bituminous coal, higher than the 69.12% found in sub-bituminous coal as shown in Table 1. In this case, the cross-linking density in sub-bituminous coal is lower [8]. Therefore, the extraction effect of the solvent is strongest with bituminous coal. With decreasing S/C ratio, the diffusion of NMP into the coal macromolecular structural network is reduced. In addition, the effect of the MI time was measured as a function of the extraction yields at certain intervals. It was found that the extraction yield increased rapidly from 0 to 10 min, but essentially no further increase in extraction yield was observed after approximately 20 min [8].

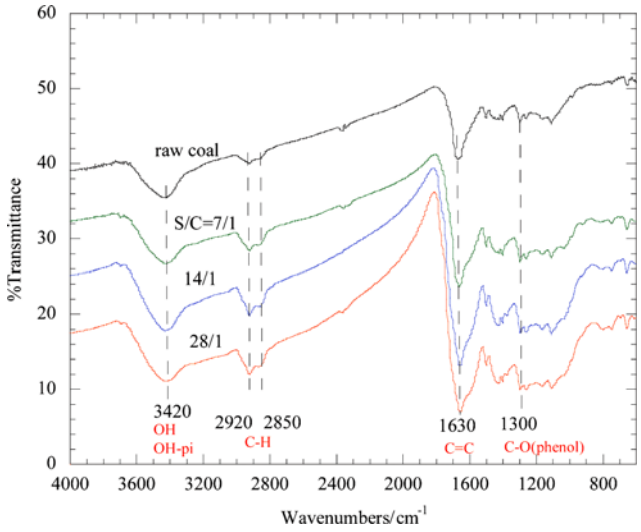

Fig. 4. FT-IR patterns of sub-bituminous raw coal and AFC1 with different S/C ratios (7 : 1, 14 : 1, 28 : 1). The AFCs were prepared by 10 min MI.

Table 1 shows that a reduction in ash of more than 99% was obtained in AFC1 by MI. The amounts of fixed carbon (FC) and volatile matter (VM) in AFC1 were higher than those for raw coal. The amount of ash obtained from AFC1 by MI was around 0.78% and from AFC2 it was 1.37%. Yoshida et al. suggested that polar solvents extract more ash materials from coals of lower rank [1]. The ash content of AFCs vary according to the method of extraction, the coal type and the solvent species. The amounts of ash obtained from AFCs by MI are lower than those obtained by thermal extraction [8].

Fig. 4 shows the FT-IR spectra of AFC1 samples with different S/C ratios. The stronger adsorption at 3,420 cm^{-1}, which is present for both AFC and raw coal, demonstrates that self-associated OH and OH-π hydrogen bonds are the main interactions [19]. The two peaks at 2,920 and 2,850 cm^{-1} are attributed to C-H bonds [20]. The peak at 1,630 cm^{-1} is mainly associated with the C=C bond in the aromatic ring. The bands around 1,300, 1,260 and 1,220 cm^{-1} for the AFC, which are assigned to C-O (phenol), C_{ar}-O-C_{ar}, C-O (alcohol) and C_{ar}-O-C_{al} structures, respectively, are stronger than those for the raw coal [19]. This suggests that more phenol and ether groups exist in the AFC. All of the above results indicate that NMP can break non-covalent interactions such as hydrogen bonds in coal, and thus extract the aromatic fractions [21].

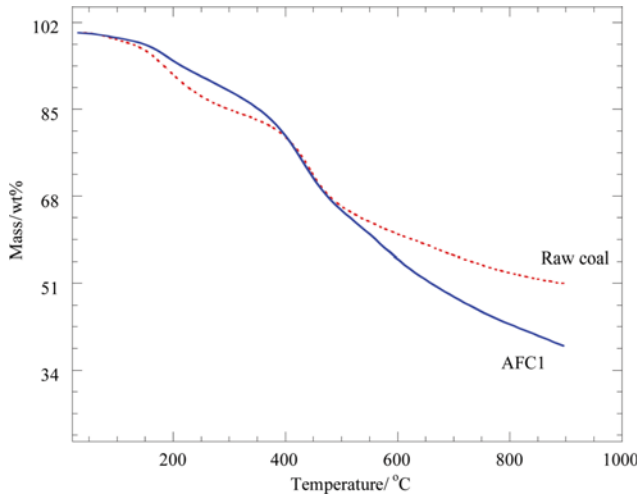

Fig. 5. TGA results of sub-bituminous raw coal and AFC1 under nitrogen conditions.

Fig. 5 shows the results from thermogravimetric analysis (TGA) of the raw sub-bituminous Arutmin coal and its AFC1 in the temperature range from 25 °C to 900 °C. At first, the slight decrease in weight of the samples at temperatures lower than 100 °C is due to desorption of moisture absorbed on the surfaces of the coal particles. Since the AFC and raw coals were dried in a vacuum oven before the measurement, the weight decreases at around 100 °C were not dominant. The weight losses at around 200 °C are due to low-temperature volatiles. The large losses at around 450 °C indicate that decomposition of organic materials takes place. The difference in weight loss between the raw coal and the AFC1 at 900 °C is as large as 12.2 wt%, which can be explained by the fact that the reduced amount of ash in the AFC allows further decomposition of organic species.

The XRD patterns for the AFCs, residues and raw coal samples are presented in Fig. 6. The diffraction profiles show the presence of a clear asymmetric (002) band around ~23° which is a similar pattern to that for the raw coal, the AFCs and also the residues. There is no obvious diffraction peak of the minerals in the XRD pattern of the organic matter, which indicates that residual inorganic matter affecting the diffraction peaks of the organic crystallite unit is not present. The position of this peak is found to shift to a higher 2θ value with increase in elemental carbon content [13,22]. The 002 peaks of the AFCs are shifted to higher 2θ values than those for the residues and raw coals. The (002) band indicates the spacing of the aromatic ring layer. In addition, the coals also contained some graphite-like structures (crystalline carbon) indicated by the presence of a clear (002) band at ~23° and a weak (100) band at ~42.3°. These observations suggest that the crystallites in all the coal samples have intermediate structures between graphite and amorphous state called turbostratic structure or random layer lattice structure [23].

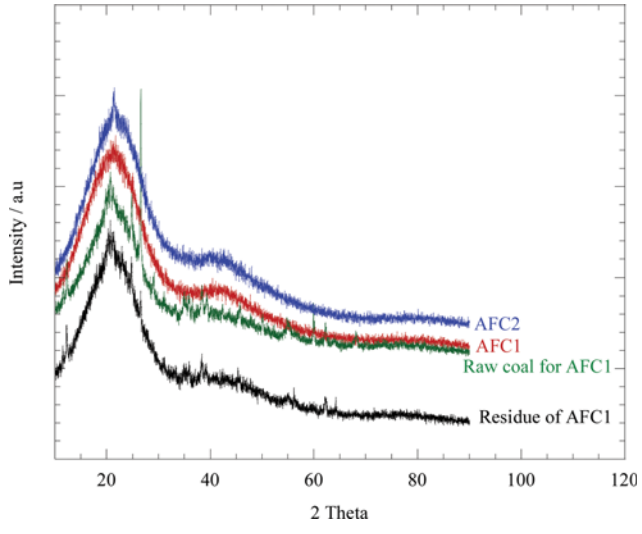

Fig. 6. XRD patterns of sub-bituminous Artumin raw coal, sub-bituminous residue, as well as AFC1 and AFC2 from bituminous Berau coal.

2. Oxidation in DCFCs

Fig. 7 compares the E_{OCV} behavior, with respect to time, for the AFCs from bituminous and sub-bituminous coals at 850 °C. During the time period from 0 to 20 s, hydrogen fuel was supplied to the anode. The E_{OCV} of H_2 fuel under these conditions is about 1.07 V. At around 20 s, the H_2 fuel supply was cut and AFC fuels were introduced to the anode with nitrogen-gas purging. At around 200 s, the E_{OCV} shows a first minimum value and at around 350 s, it has a second minimum value. The first increase in E_{OCV}, from 220 to 300 s, could be attributed to H_2 production, whereas the second increase, from 350 s onwards, could be attributed to CO production [18,24]. After 900 s, the E_{OCV} decreased slightly, which indicated decreases in the CO and hydrogen compositions. This may depend on the volatile matter, and the liquid-like state of the AFC at high temperatures might affect the cell performance [6]. However, the reasons for this phenomenon may be complicated and are not well understood. The results imply that the use of AFC as a fuel results in a higher cell voltage than carbon made from bamboo [25].

The similarity of the open-circuit voltages for AFC1 and AFC2

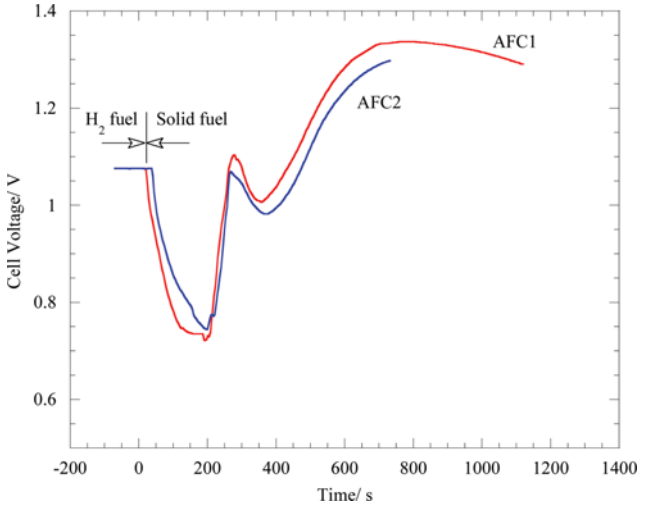

Fig. 7. Time dependence of the E_{OCV} of the AFC/electrolyte fuel (3 g/3 g) at 850 °C.

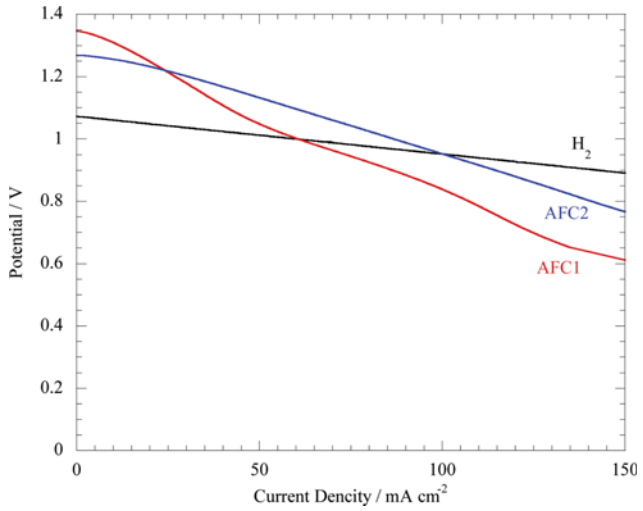

Fig. 8. Comparison of the current-voltage behavior of H_2 fuel and AFC fuels (AFC/electrolyte=3 g/3 g) at 850 °C.

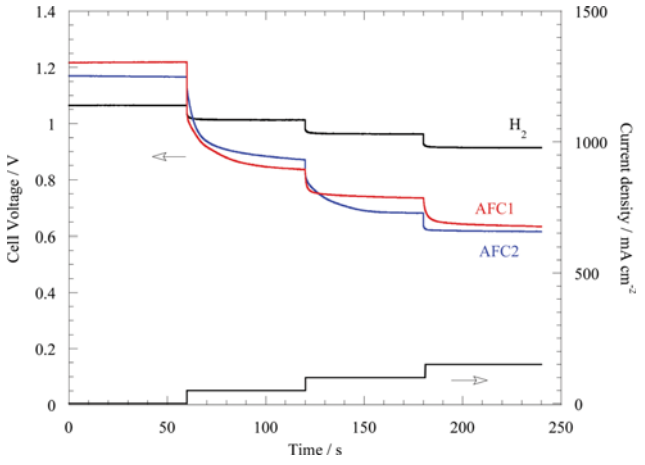

Fig. 9. SC behavior at the current steps with H_2 fuel and AFC fuels (AFC/electrolyte=3 g/3 g) at 850 °C.

is shown in Fig. 7. In particular, the two above-mentioned voltage decreases indicate that the coals are gasified and that the gasification of the AFCs is similar, regardless of the raw coal species. However, the E_{OCV} of AFC1 is slightly higher than that of AFC2. As the E_{OCV} is determined by gas partial pressures and temperature, i.e., by thermodynamic reasons, this difference could be attributed to different gas partial pressures. Therefore, the higher voltage of AFC1 indicates that AFC1 from Arutmin coal provides a larger H_2 or CO partial pressure and less CO_2 than AFC2 from Berau coal.

Fig. 8 compares the voltage-current behavior of AFCs and hydrogen fuel (0.125 L min^{-1} H_2/0.025 L min^{-1} CO_2 with ca. 5% H_2O) at a potential scan rate of 0.25 mV s^{-1} at 850 °C. The E_{OCV} of hydrogen fuel is about 1.07 V at 850 °C as mentioned above. It is observed that the slopes for AFC fuels are much steeper than for H_2 fuel, especially in the high current density region. This indicates that AFC fuels have higher reaction and mass transfer resistances than hydrogen fuel. The maximum E_{OCV} of AFC1 was 1.35 V and of AFC2 was 1.26 V at 850 °C. The high E_{OCV} values of the AFCs at high temperature are in agreement with previous results [25-27]. Lee et al. reported that the anode has a very high exchange-current density, and thus the anode reaction is a gas-phase mass transfer-controlled process [17]. In addition, the mass transfer resistance depends on the flow rates of H_2, CO_2 and H_2O. A previous study [6] reported that AFC produced approximately 45 mol% H_2 and 50 mol% CO. Thus, it is plausible that a larger amount of CO disturbs H_2 transport to the electrode surface, resulting in higher resistance of the AFCs in the anode.

AFC1 shows a slightly steeper slope than AFC2, as shown in Fig. 8. This means that AFC1 has a larger oxidation resistance in the anode. As mentioned above, the anode reaction is mostly a mass transfer-controlled process; thus less H_2 and CO from AFC1 may result in a larger resistance than for AFC2 in the anode. Indeed, solid carbon is gasified to H_2 and CO gases. However, the gasification process may not be constant and the irregular gas generation behavior of the AFCs may result in less gas being generated from AFC1 although AFC1 has a higher E_{OCV} than AFC2.

Fig. 9 shows the SC results for AFC fuels (3 g AFC/3 g Li-K carbonates) and H_2 fuel at 850 °C. The SC results show voltage relaxation with the current step, which represents the kinetic and mass transfer behavior of the reaction system; slow relaxation indicates low diffusivity and slow mass transfer of the reaction species. Fig. 9 shows that the hydrogen fuel has a smaller voltage step and faster voltage relaxation than AFC fuels. During the current steps to 50, 100 and 150 mA cm^{-2}, the voltage steps of hydrogen fuel (ΔE) are similar at around 0.1 V, indicating that hydrogen fuel reaches a steady state very fast and has high diffusivity and activity. On the other hand, AFC fuels have a slow decline in voltage, showing unstable voltage relaxation, especially at the first step from 0 to 50 mA cm^{-2}. At the first current step, the voltage drops significantly from 1.21 to 0.85 V (ΔE_1=0.36 V). Thus, the voltage gap at the first current step (ΔE_1) is much greater than that at the second (ΔE_2) and third voltage (ΔE_3) gaps, which result in voltage drops of ΔE_2=ΔE_3=0.13 V. The reason why the first voltage gap is much larger than the second and third gaps is unclear at this stage. If slow relaxation at the first voltage gap is related to activation polarization caused by slow charge transfer, then the current-voltage behavior in Fig. 8 should represent a steep decrease near to zero current for the AFC fuels. However, the current-voltage behavior exhibits a linear decrease with applied current. This behavior could be strongly connected to the gasification of the solid fuel, the gas transport paths through the porous solids as well as fuel oxidation at the porous electrode. In addition, negligible differences in oxidation between the AFCs are indicated by these SC results.

CONCLUSION

AFCs of Arutmin sub-bituminous coal and Berau bituminous coal were successfully prepared using microwave irradiation. Raw coals were extracted under conditions of 202 °C and atmospheric pressure, and the following conclusions can be drawn:

(i) As a strong polar solvent, NMP is the best polar solvent and could successfully perform the extraction. The extraction ability of NMP is higher than DMA, DMF and DMSO.

(ii) The extractability of Berau coal is higher than that of Arut-

min coal. The highest extraction yield of Arutmin coal in NMP was 23.53% and that of Berau was 33.80% at 202 °C and atmospheric pressure. The ash content of the AFCs was reduced to about one-tenth of that in the raw coal.

(iii) The oxidation behavior of the different AFCs in a DCFC was similar. The DCFC ran successfully with the AFCs at 850 °C. The E_{OCV} of the AFCs were about 1.35 V for Arutmin coal and 1.26 V for Berau coal at 850 °C. The voltage outputs were 0.61 V for AFC1 and 0.74 V for AFC2 at a current density of 150 mA cm^{-2}. These results support the hypothesis that the performance of AFCs would be indistinguishable, regardless of the raw coal species.

(iv) The AFCs showed a steeper slope than hydrogen fuel in the current-voltage plot, indicating that the AFC had a larger resistance than hydrogen in the oxidation. A possible reason is that the high content of CO in the anode obstructs mass transfer of H_2 species.

ACKNOWLEDGEMENT

This research was supported by Basic Science Research Program through the National Research Foundation of Korea (NRF) funded by the Ministry of Education, Science and Technology (2011-0009748).

REFERENCES

1. T. Yoshida, T. Takanohashi, K. Sakanishi, I. Saito, M. Fujita and K. Mashimo, *Energy Fuels*, **16**, 1006 (2002).
2. C. Li, T. Takanohashi, I. Saito, M. Iino, H. Aoki and K. Mashimo, *Energy Fuels*, **18**, 97 (2004).
3. M. Muthuvel, X. Jin, G. G. Botte in Encyclopedia Electrochemical Power Sources, Vol. 3 (Eds. Jurgen Garche), ELSEVIER, Netherlands, pp. 158 (2009).
4. S. D. Kim, K. J. Woo, S. K. Jeong, Y. J. Rhim and S. H. Lee, *Korean J. Chem. Eng.*, **25**, 758 (2008).
5. N. Okuyama, N. Komatsu, T. Shigehisa, T. Kaneko and S. Tsuruya, *Fuel Process. Technol.*, **85**, 947 (2004).
6. J. P. Kim, H. Lim, C. H. Jeon, Y. J. Chang, K. N. Koh and S. M. Choi, *Int. J. Hydrogen Energy*, **37**, 11401 (2012).
7. N. Kashimura, T. Takanohashi and I. Saito, *Energy Fuels*, **20**, 2063 (2006).
8. Ö. Sönmez and E. S. Giray, *Fuel*, **90**, 2125 (2011).
9. H. Shui, Y. Zhou, H. Li, Z. Wang, Z. Lei, S. Ren, C. Pan and W. Wang, *Fuel*, **108**, 385 (2013).
10. D. X. Cao, Y. Sun and G. L. Wang, *J. Power Sources*, **167**, 250 (2007).
11. X. Li, Z. H. Zhu, J. L. Chen, R. D. Marco and A. Dicks, *J. Power Sources*, **186**, 1 (2009).
12. J. R. Selman, *J. Power Sources*, **156**, 128 (2006).
13. C. G. Lee, H. Hur and M. B. Song, *J. Electrochem. Soc.*, **158**, B410 (2011).
14. A. L. Dicks, *J. Power Sources*, **156**, 128 (2006).
15. N. J. Cherepy, R. Krueger, K. J. Fiet, A. F. Jankowski and J. F. Cooper, *J. Electrochem. Soc.*, **152**, A80 (2005).
16. W. H. A. Peelen, M. Olivry, S. F. Au, J. D. Fehribach and K. Hemmes, *J. Appl. Electrochem.*, **30**, 1389 (2000).
17. C. G. Lee, *Fuel Cells*, **12**, 550 (2012).
18. C. G. Lee and W. K. Kim, Proc. 224th ECS meeting, San Francisco, No. 747 (2013).
19. Z. Lei, L. Wu, Y. Zhang, H. Shui, Z. Wang, C. Pan, H. Li, S. Ren and S. Kang, *Fuel*, **95**, 630 (2012).
20. M. Rahman, A. Samanta and R. Gupta, *Fuel Process. Technol.*, **115**, 88 (2013).
21. K. Renganathan and J. W. Zondlo, *Fuel Sci. Technol. Int.*, **11**, 677 (1993).
22. T. Ungar, J. Gubicza, G. Ribarik, C. Pantea and T. W. Zerda, *Carbon*, **40**, 929 (2002).
23. P. N. Vishwakarma, V. Prasad, S. V. Subramanyam and V. Ganesan, *Bull. Mater, Sci.*, **28**, 609 (2005).
24. J. Zhang, Z. Zhong, D. Shen, J. Zhao, H. Zhang, M. Yang and W. Li, *Energy Fuels*, **25**, 2187 (2011).
25. J. P. Kim, H. Lim, C. H. Jeon, Y. J. Chang, K. N. Koh and S. M. Choi, *J. Power Sources*, **195**, 7568 (2010).
26. A. Elleuch, A. Boussetta and K. Halouani, *J. Electroanal. Chem.*, **668**, 99 (2012).
27. J. Ruflin, A. D. Perwich II, C. Brett, J. K. Berner and S. M. Lux, *J. Power Sources*, **213**, 275 (2012).